Photodynamic Therapy

DOI: 10.1002/anie.201104765

Mannose-Functionalized Mesoporous Silica Nanoparticles for Efficient Two-Photon Photodynamic Therapy of Solid Tumors**

Magali Gary-Bobo, Youssef Mir, Cédric Rouxel, David Brevet, Ilaria Basile, Marie Maynadier, Ophélie Vaillant, Olivier Mongin, Mireille Blanchard-Desce, Alain Morère, Marcel Garcia,* Jean-Olivier Durand,* and Laurence Raehm*

In the context of national systematic screenings for cancer, photodynamic therapy (PDT) has arisen as an alternative to chemo- and radiotherapy for the non-invasive selective destruction of small tumors. PDT involves the use of a photosensitizer which, upon irradiation at specific wavelengths, in the presence of oxygen, leads to the generation of cytotoxic species and consequently to irreversible cell damage.[1] PDT combined with two-photon excitation (TPE)[2,3] in the near-IR region offers new perspectives for the treatment of solid tumors owing to its increased penetration depth and unique spatial resolution. However, the use of conventional photosensitizers requires very high excitation powers[4] (close to the threshold of tissue photodamage) because of the low two-photon absorption (TPA) cross-sections (σ_2) in the biological spectral window (i.e. 700–1000 nm). The design of novel photosensitizers having much larger TPA cross-sections is thus crucial. Up until recently, very few examples of TPE-PDT in vivo with photosensitizers having large cross-sections have been reported.[5–7] Collins et al.[7] and Khurana et al.[5] have established that TPE-PDT using novel biphotonic photosensitizers derived from porphyrin dimers was efficient for blood vessel closure in mice. Starkey et al.[6] confirmed the efficiency of TPE-PDT for the destruction of breast and lung cancer xenografts in mice down to a depth of 2 cm, using photosensitizers specifically engineered for TPE.

To enhance the selectivity towards tumor cells and the efficiency of PDT, the encapsulation of photosensitizers in nanoparticles is a promising route that has stimulated tremendous efforts.[8–10] However, the nanoparticle approach is still in its infancy for TPE-PDT, as only three relevant in vitro studies have been reported so far,[11–13] while in vivo results are still missing. In addition, reported in vitro studies deal with nanoparticles that have not been functionalized with targeting biomolecules. The use of biomolecules is particularly important to increase the therapeutic efficiency of nanoparticles both in vitro and in vivo.[14,15] The photosensitizers used for PDT and TPE-PDT are also sensitive to excitation by UV/visible light; this serious drawback leads to the prolonged sensitivity of the patient to sunlight and entails post-treatment precautions.

Mesoporous silica nanoparticles (MSNs) hold great promise for cancer therapy as they are biocompatible and preferentially accumulate in tumors.[16–18] Following our earlier work dealing with the elaboration of fluorescent MSNs with giant TPA cross-sections,[19–21] we report herein on original MSNs for efficient TPE-PDT. The MSN surface was postfunctionalized with a mannose derivative in order to target lectins over-expressed by cancer cells.[14] Incubated with cancer cells, these MSNs were nontoxic under daylight illumination. TPE-PDT with these MSNs was investigated in vitro on human breast and colon cancer cell lines. In vivo experiments were also performed on athymic mice bearing xenografted tumors from colon cancer cells.

Here we show that the photosensitizer **PS**[22] was covalently encapsulated inside MSNs following the method described earlier[14] for porphyrin derivatives. **MSN1**, incorporating 6850 units of **PS** per nanoparticle and having a hydrodynamic diameter of 118 nm, was synthesized. Grafting of the mannose moiety on the surface yielded **MSN1-mannose** (Scheme 1). The TPA properties of **PS** are retained in the MSNs (see Table 2 and Figure 2 in the Supporting Information), with 1200 GM (Göppert–Mayer units, 1 GM = 10^{-50} cm^4 s photon^{-1} molecule^{-1}) per **PS** thus leading to giant

[*] Dr. M. Gary-Bobo, Dr. I. Basile, Dr. M. Maynadier, O. Vaillant, Prof. A. Morère, Dr. M. Garcia
Institut des Biomolécules Max Mousseron
UMR 5247 CNRS-UM1-UM2
Faculté de Pharmacie, Avenue Charles Flahault
34093 Montpellier Cedex 05 (France)
E-mail: marcel.garcia@inserm.fr

Dr. Y. Mir, Dr. C. Rouxel, Dr. O. Mongin, Dr. M. Blanchard-Desce
Chimie et Photonique Moléculaires, CNRS UMR 6510
Campus de Beaulieu, Université Rennes 1
35042 Rennes Cedex (France)
E-mail: mireille.blanchard-desce@univ-rennes1.fr

Dr. D. Brevet, Dr. J.-O. Durand, Dr. L. Raehm
Institut Charles Gerhardt Montpellier
UMR 5253 CNRS-UM2-ENSCM-UM1, CC1701
Place Eugène Bataillon, 34095 Montpellier Cedex 05 (France)
E-mail: durand@univ-montp2.fr

[**] Financial support by ANR PNANO. (07-102), ARC (no. SFI20101201906), and the nonprofit organization Rétinostop is gratefully acknowledged. Région Bretagne provided a fellowship to C.R., M.M. was supported by Montpellier 2 University, and O.V. was supported by the "Ligue Nationale contre le Cancer". We thank Emmanuel Schaub, PIXEL platform (Multiphotonic Microscopy Facilities, University of Rennes 1), Michel Gleizes for histogical sample treatments, the Montpellier RIO imaging platform, Fabrice Senger for expert assistance in conducting TPE-PDT experiments, Céline Frochot for $^1O_2$ quantum yield measurements, and R. Freydier and J. L. Seidel for silicon analyses by ICP-MS ("AETE" Analytical Regional Platform Facilities, OREME observatory of Montpellier 2 University).

Supporting information for this article is available on the WWW under http://dx.doi.org/10.1002/anie.201104765.

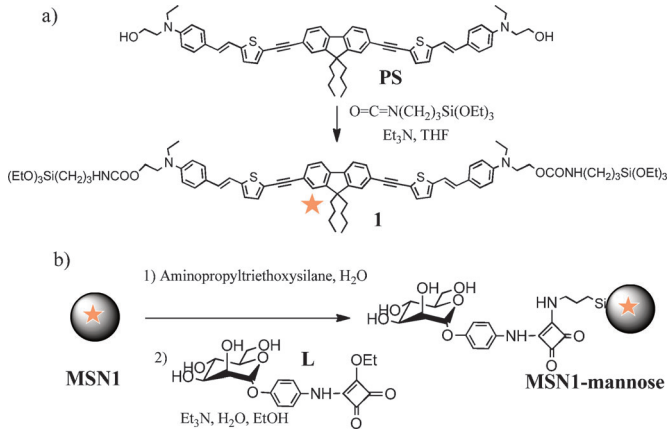

Scheme 1. a) Synthesis of **1** and b) Synthesis of nanoparticles **MSN1-mannose**.

TPA cross-sections (up to 8 MGM) for a single MSN. In contrast to **PS** in solution, MSNs showed no detectable singlet oxygen emission at 1270 nm when excited either at 430 nm or in the UV region. Such an effect can be ascribed to light scattering as well as to the screening effect of the surface linker groups (see the Supporting Information) for **MSN1-mannose** nanoparticles. Both phenomena prevent excitation of inner **PS** and explain the absence of toxicity of MSNs under standard (such as daylight) illumination (vide infra). In contrast, because of the significant scattering ($\propto 1/\lambda^4$) reduction at long wavelengths and the high contrast between TPA cross-sections of **PS** and surface linker groups (see the Supporting Information), TPE of **MSN1-mannose** in the near-IR region is expected to be both effective and selective, thus opening a promising route for therapy by TPE in the near-IR region.

TPE-PDT experiments were performed with **MSN1-mannose** using three distinct cancer cell lines (breast cancer cell lines MCF-7 and MDA-MB-231, and the colon cancer cell line HCT-116). As evident in Table 1, the photodynamic therapeutic potential of the MSNs functionalized with mannose (**MSN1-mannose**) is clearly higher than that of unfunctionalized nanoparticles (**MSN1**). This can be explained by the presence of mannose receptors on MCF-7[23] and MDA-MB-231[14] breast cancer cells. The most important cytotoxic effect was observed with the colorectal cancer cell line (HCT-116). The high interest for lectin targeting for this type of cancer[24] is demonstrated here (Figure 3 in the Supporting Information) by the 2–5-fold higher uptake of fluorescein-labeled mannose-functionalized MSN (**MSN-FITC-mannose**)[25] in HCT-116 cells relative to that of MCF-7 and MDA-MB-231 cells and normal fibroblasts, and by the finding of a typical overexpression of one of the mannose receptors, MRC2 (mannose receptor C-type 2), in these cells. Note that PDT efficiency depends on the incubation time with **MSN1-mannose**, since after 24 h of incubation (and irradiation as described above) 100 % of the MCF-7 cells were lysed (Figure 1 a). Interestingly, as a consequence of the highly confined excitation provided by TPE using focused excitation, cell death was observed only in the irradiated area, and neighboring MDA-MB-231 cells were not affected (Figure 1 b). Importantly, the nanoparticles were found to be nontoxic without irradiation (Table 1) while irradiation alone did not damage the cells (data not shown). In addition, no cell death was observed when the cells were exposed to daylight up to 4 h, indicating that multifunctionalized MSNs are nontoxic under standard illumination conditions (see Table 4 and Figure 4 in the Supporting Information). These characteristics open a new avenue for improved PDT protocols using multifunctionalized MSNs that act as potent photosensitizers only under TPE in the NIR, allowing high spatial precision of cell lyses while reducing unwelcome effects such as sensitization under daylight exposition.

Table 1: In vitro photodynamic efficiency.[a]

With irradiation		Living cells [%]	
treatment	MCF-7	MDA-MB-231	HCT-116
control	100 ± 17	100 ± 17	100 ± 11
MSN1	64 ± 18[b]	67 ± 6[b]	50 ± 6[b]
MSN1-mannose	44 ± 4[c]	33 ± 15[c]	27 ± 10[c]
Without irradiation		**Living cells [%]**	
treatment	MCF-7	MDA-MB-231	HCT-116
control	100 ± 6	100 ± 4	100 ± 6
MSN1	105 ± 10	105 ± 10	99 ± 2
MSN1-mannose	101 ± 8	101 ± 8	98 ± 3

[a] Two breast cancer cell lines (MCF-7 and MDA-MB-231) and a colon cancer cell line (HCT-116) were incubated for 4 h with 20 μg mL^{-1} of **MSN1** or **MSN1-mannose**. After renewal of the culture medium, cells were irradiated at 760 nm (3 × 1 s) using a confocal microscope equipped with a mode-locked Ti:sapphire laser generating 100 fs wide pulses at a rate of 80 MHz. The laser beam was focused by a microscope objective lens (10×, NA 0.4). The wells were irradiated at 760 nm by three successive scans of 1 s duration each at an average power of 80 mW. The surface of the scanned areas was 1.5 × 1.5 mm^2 (mean energy of 10.6 J cm^{-2}). Living cells were determined by MTT assay 2 days after irradiation. Values represent the mean ± standard deviation of three experiments. [b, c] Statistically different (Student's t test): [b] $p < 0.05$ from control, [c] $p < 0.01$ from **MSN1**.

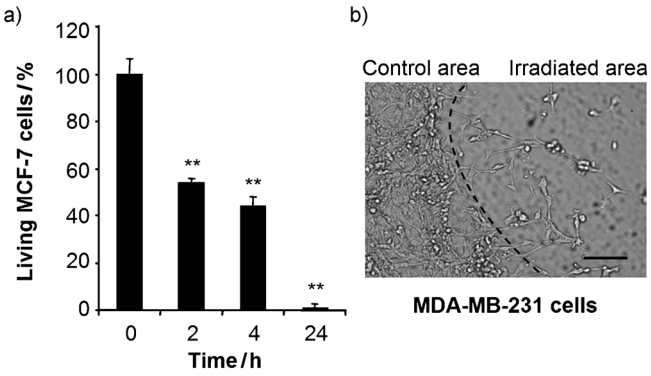

Figure 1. TPE-PDT efficacy with **MSN1-mannose.** a) Confluent MCF-7 cells were irradiated at 760 nm for 3 s after the indicated times of treatment with **MSN1-mannose** (20 μg mL^{-1}). Error bars represent standard deviation. b) An optical microscope image of MDA-MB-231 cancer cells incubated for 24 h with **MSN1-mannose** (20 μg mL^{-1}) and then submitted to two-photon irradiation only on a part of the well. Cell death was observed after 2 days and occurred in the irradiated area only. Scale bar, 25 μm.

Based on in vitro results, we then examined TPE-PDT in vivo, on nude mice bearing HCT-116 xenografts. Twelve mice were subcutaneously injected in the flank with HCT-116 cells. Fifteen days after cancer cell injection, three uniform mice groups (4, 4, 3) bearing subcutaneous tumors with a mean tumor volume of 27 mm^3 were selected. Three mice were injected intravenously with 200 μL of saline solution (0.9% NaCl) and eight mice with **MSN1-mannose** (16 mg kg^{-1}). Three hours later, four of the eight mice injected with **MSN1-mannose** were anesthetized and tumors were submitted to two-photon irradiation at 760 nm for three periods of 3 min and light was focused on three different tumor areas. The xenografts were localized at a tissue depth between 1 and 4 mm.

Thirty days after treatment, the mice were sacrificed, and the tumors were removed and measured. Results reported in Table 2 and Figure 2 showed a strong reduction in tumor weight (ca. 70%) for the four mice treated with **MSN1-mannose** and submitted to TPE-PDT in comparison to the tumors of the three mice treated with saline solution alone and the four mice treated with **MSN1-mannose** but not submitted to subsequent irradiation. No mortality was observed for the 30 days following the injection of **MSN1-mannose**, suggesting that these nanoparticles are not toxic except in the tumor area under TPE. After sacrifice of the mice, we examined the development of clinically detectable macrometastases connected with the invasive potential of HCT-116 cancer cells. As shown in Table 2, **MSN1-mannose** treatment followed by TPE-PDT prevented macrometastasis formation in liver and colon in comparison to the groups of mice treated with saline alone or with **MSN1-mannose** without irradiation. This effect can most probably be related to the decrease of the subcutaneous tumor growth and of its associated neoangiogenesis, both of which delay the spread of cancer cells and subsequent distal metastasis.

Table 2: Effect of TPE-PDT on tumor and metastasis formation.[a]

Treatment	Mice group	Tumor weight [g]	Mice with metastases to liver	to colon
control	3	1.39 ± 0.49	3	2
MSN1-mannose	4	1.33 ± 0.72	2	2
MSN1-mannose + 2 *hν* irradiation	4	0.40 ± 0.28[b]	0	0

[a] Measurements[26] were made 30 days after treatment with saline solution (control) alone or with **MSN1-mannose** (dose = 16 mg kg^{-1}) followed (or not) by laser irradiation at 760 nm, 3 × 3 min at 80 mW (mean energy of 3 × 640 J cm^{-2} for a surface of 1.5 × 1.5 mm^2). For tumor weight, values represent mean ± standard deviation. The number of mice in each group developing liver or colon metastases (> 2 mm) is indicated. [b] $p < 0.05$ statistically different from control (*t* test).

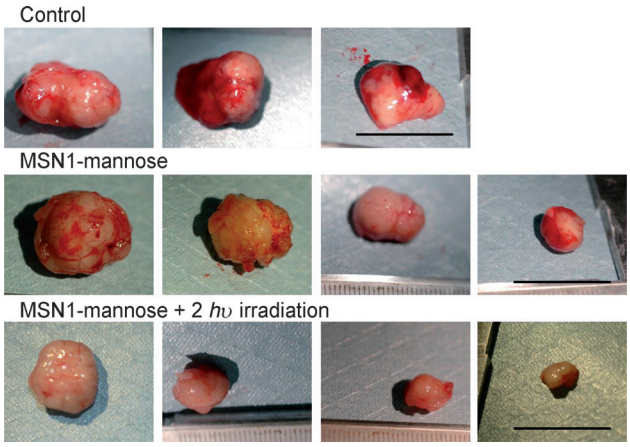

Figure 2. Effect of TPE-PDT on tumor growth. Photographs of tumors described in Table 2. Tumors were dissected from mice 30 days after treatment with saline (control) or **MSN1-mannose** (16 mg kg^{-1}) followed (or not) by TPE-PDT as described. Scale bars, 2 cm.

As **MSN1-mannose** may induce subsequent damage in the organs involved in their clearance, systemic and organ-specific toxicities were investigated. The renal clearance of the **MSN1-mannose**, evaluated by silicon detection by inductively coupled plasma mass spectrometry (ICP-MS), was maximal at 7–8 days and the cumulative recovery in urine after 13 days superior to 80% of the injected Si (Figure 3a).

The weights of the mice treated with **MSN1-mannose** were not statistically different from those of the control mice; for both groups the weight ratios of liver, spleen, kidney over body weight were comparable (see Table 5 in the Supporting Information). Conventional biomarkers representative for tissue functionality and/or systemic inflammation such as creatinine (renal function), ALT (liver function), and TNFα and IL-6 (systemic toxicity) appeared unmodified over the two weeks following nanoparticle injection (Figure 3b–e). Histological examinations of livers, spleens, and kidneys indicated no apparent abnormalities or lesions 14 days after **MSN1-mannose** treatment (Figure 3f).

In conclusion, we have described the first example of tumor treatment using carbohydrate-functionalized MSNs phototriggered by two-photon irradiation in the near IR and without toxicity under standard (daylight) illumination. This study demonstrated that a single injection was sufficient to target these nanoparticles to the tumor area while two-photon irradiation in the near IR induced a major reduction of the tumor size. In addition, this protocol was shown to impair the development of metastases associated with the spread of cancer without apparent systemic toxicity. This therapeutic approach holds great promise and appears particularly appropriate for the minimally invasive ablation of small localized solid tumors (prostate and colon cancers, retinoblastoma, head and neck cancers) whose detection has dramatically increased with routine cancer screening programs.[27] A focal and targeted TPE-PDT could thus provide an alternative to conventional more invasive or harsher therapies (such as surgery and radiotherapy) for organ-confined and low-grade diseases.[28]

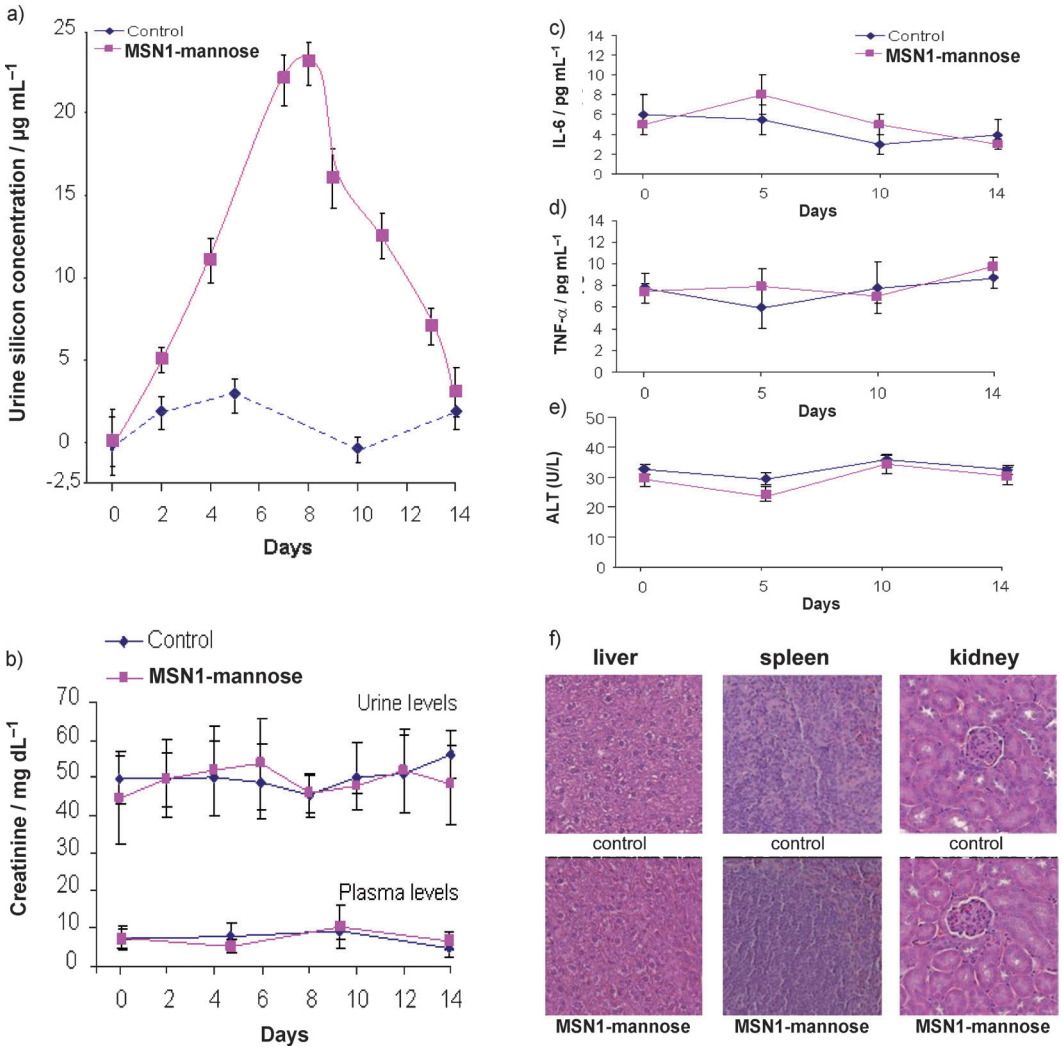

Figure 3. Renal clearance and biocompatibility of **MSN1-mannose.** a) Renal clearance of nanoparticles was evaluated over a period of two weeks after intravenous injection of 16 mg kg^{-1} **MSN1-mannose**. Silicon concentration was determined at different times in the urine of mice injected with nanoparticles ($n = 5$, MSN-treated group, ■) and in mice injected with PBS ($n = 5$, control group, ◆) by ICP-MS. b–e) Toxicity evaluation of **MSN1-mannose**. The concentrations of several biological markers for systemic toxicity were evaluated in control (◆) and **MSN1-mannose**-treated mice (■) described in (a). b) Creatinine activity was evaluated in urine. Expression of IL-6 (c) and TNFα (d) was quantified in serum by specific ELISA immunoassays, and expression of ALT (alanine aminotransferase was quantified by enzymatic assay. Error bars in (a–e) indicate standard deviation. f) Hematoxylin- and eosin-stained sections from paraffin-embedded tissues of control and treated mice were examined by a pathologist. Scale bars, 50 µm.

Experimental Section

TPE-PDT in vitro: For cell culture, MDA-MB-231 and MCF-7 human breast cancer cells and normal human fibroblasts (ATCC) were routinely cultured in Dulbecco's modified Eagle's medium (DMEM) supplemented with 10% fetal bovine serum and 50 µg mL^{-1} gentamycin. HCT-116 human colorectal cancer cells (ATCC) were cultured in McCoy culture medium supplemented with 10% fetal bovine serum and 50 µg mL^{-1} gentamycin. All these cell types were allowed to grow in humidified atmosphere at 37°C under 5% CO_2.

For in vitro phototoxicity, MDA-MB-231, MCF-7, and HCT-116 cells were seeded into a 384 multiwell glass-bottomed plate (thickness 0.17 mm), with a black polystyrene frame, 2000 cells per well in 50 µL of culture medium, and allowed to grow for 24 h. Cells were then incubated for 4 h with or without 20 µg mL^{-1} of MSNs. After incubation with MSNs, cells were washed twice, maintained in fresh culture medium, and then submitted (or not) to laser irradiation; scanned area: 1.5 × 1.5 mm^2. The entire area of the well was irradiated at 760 nm by three scans of 1 s duration. The average power delivered to the sample was measured with a thermoelectric optical energy meter and was 80 mW. The laser beam was focused by a microscope objective lens (10×, NA 0.4).

For kinetic experiments, MCF-7 cells were incubated for 2, 4, and 24 h with or without 20 µg mL^{-1} of **MSN1-mannose**. After incubation, cells were washed twice, maintained in fresh culture medium, and then submitted (or not) to laser irradiation.

TPE-PDT in vivo: Animal experiments were approved and conducted in accordance with local and national authorities for the care and use of laboratory animals. For in vivo photodynamic therapy experiments, 12 female Swiss nude mice (six-weeks-old; from Charles River) were xenografted in the flank by a subcutaneous injection of 100 µL of a monocellular suspension containing 10^6 HCT-116 cells and a reconstituted extracellular matrix (Matrigel 5 mg mL^{-1}). Fifteen days after cancer-cell injection, 11 mice were injected intravenously in

the tail vein, with 200 μL of physiological serum added (or not) with **MSN1-mannose** (16 mg kg^{-1}). Three hours after the injection, four mice, which had been injected with **MSN1-mannose**, were anesthetized (2,2,2-tribromoethanol), and their tumors were submitted to two-photon irradiation at 760 nm through a 1 mm glass slide for three periods of 3 min (separated by 3 min lag time) at three different areas of the tumor. Thirty days after this treatment, the mice were sacrificed and tumors were removed and measured.

Received: July 8, 2011
Published online: October 4, 2011

Keywords: antitumor agents · nanoparticles · photodynamic therapy

[1] C. A. Robertson, D. H. Evans, H. Abraharnse, *J. Photochem. Photobiol. B* **2009**, *96*, 1 – 8.
[2] W. Denk, J. H. Strickler, W. W. Webb, *Science* **1990**, *248*, 73 – 76.
[3] C. Xu, W. Zipfel, J. B. Shear, R. M. Williams, W. W. Webb, *Proc. Natl. Acad. Sci. USA* **1996**, *93*, 10763 – 10768.
[4] K. S. Samkoe, A. A. Clancy, A. Karotki, B. C. Wilson, D. T. Cramb, *J. Biomed. Opt.* **2007**, *12*, 034025.
[5] M. Khurana, E. H. Moriyama, A. Mariampillai, K. Samkoe, D. Cramb, B. C. Wilson, *J. Biomed. Opt.* **2009**, *14*, 064006.
[6] J. R. Starkey, A. K. Rebane, M. A. Drobizhev, F. Q. Meng, A. J. Gong, A. Elliott, K. McInnerney, C. W. Spangler, *Clin. Cancer Res.* **2008**, *14*, 6564 – 6573.
[7] H. A. Collins, M. Khurana, E. H. Moriyama, A. Mariampillai, E. Dahlstedt, M. Balaz, M. K. Kuimova, M. Drobizhev, V. X. D. Yang, D. Phillips, A. Rebane, B. C. Wilson, H. L. Anderson, *Nat. Photonics* **2008**, *2*, 420 – 424.
[8] D. Bechet, P. Couleaud, C. Frochot, M.-L. Viriot, F. Guillemin, M. Barberi-Heyob, *Trends Biotechnol.* **2008**, *26*, 612 – 621.
[9] D. K. Chatterjee, L. S. Fong, Y. Zhang, *Adv. Drug Delivery Rev.* **2008**, *60*, 1627 – 1637.
[10] P. Couleaud, V. Morosini, C. Frochot, S. Richeter, L. Raehm, J. O. Durand, *Nanoscale* **2010**, *2*, 1083 – 1095.
[11] D. Gao, R. R. Agayan, H. Xu, M. A. Philbert, R. Kopelman, *Nano Lett.* **2006**, *6*, 2383 – 2386.
[12] S. Kim, T. Y. Ohulchanskyy, H. E. Pudavar, R. K. Pandey, P. N. Prasad, *J. Am. Chem. Soc.* **2007**, *129*, 2669 – 2675.
[13] M. Velusamy, J. Y. Shen, J. T. Lin, Y. C. Lin, C. C. Hsieh, C. H. Lai, C. W. Lai, M. L. Ho, Y. C. Chen, P. T. Chou, J. K. Hsiao, *Adv. Funct. Mater.* **2009**, *19*, 2388 – 2397.
[14] D. Brevet, M. Gary-Bobo, L. Raehm, S. Richeter, O. Hocine, K. Amro, B. Loock, P. Couleaud, C. Frochot, A. Morere, P. Maillard, M. Garcia, J. O. Durand, *Chem. Commun.* **2009**, 1475 – 1477.
[15] Y. E. L. Koo, G. R. Reddy, M. Bhojani, R. Schneider, M. A. Philbert, A. Rehemtulla, B. D. Ross, R. Kopelman, *Adv. Drug Delivery Rev.* **2006**, *58*, 1556 – 1577.
[16] H. Meng, M. Xue, T. Xia, Z. Ji, D. Y. Tarn, J. I. Zink, A. E. Nel, *Acs Nano* **2011**, *5*, 4131 – 4144.
[17] V. Mamaeva, J. M. Rosenholm, L. T. Bate-Eya, L. Bergman, E. Peuhu, A. Duchanoy, L. E. Fortelius, S. Landor, D. M. Toivola, M. Linden, C. Sahlgren, *Mol. Ther.* **2011**, *19*, 1538 – 1546.
[18] J. Lu, M. Liong, Z. Li, J. I. Zink, F. Tamanoi, *Small* **2010**, *6*, 1794 – 1805.
[19] V. Lebret, L. Raehm, J. O. Durand, M. Smaihi, M. H. V. Werts, M. Blanchard-Desce, D. Methy-Gonnod, C. Dubernet, *J. Biomed. Nanotechnol.* **2010**, *6*, 176 – 180.
[20] V. Lebret, L. Raehm, J. O. Durand, M. Smaihi, M. H. V. Werts, M. Blanchard-Desce, D. Methy-Gonnod, C. Dubernet, *J. Sol-Gel Sci. Technol.* **2008**, *48*, 32 – 39.
[21] V. Lebret, L. Raehm, J. O. Durand, M. Smaihi, C. Gerardin, N. Nerambourg, M. H. V. Werts, M. Blanchard-Desce, *Chem. Mater.* **2008**, *20*, 2174 – 2183.
[22] C. Rouxel, M. Charlot, Y. Mir, C. Frochot, O. Mongin, M. Blanchard-Desce, *New J. Chem.* **2011**, *35*, 1771 – 1780.
[23] D. Wienke, G. C. Davies, D. A. Johnson, J. Sturge, M. B. K. Lambros, K. Savage, S. E. Elsheikh, A. R. Green, I. O. Ellis, D. Robertson, J. S. Reis-Filho, C. M. Isacke, *Cancer Res.* **2007**, *67*, 10230 – 10240.
[24] T. Minko, *Adv. Drug Delivery Rev.* **2004**, *56*, 491 – 509.
[25] O. Hocine, M. Gary-Bobo, D. Brevet, M. Maynadier, S. Fontanel, L. Raehm, S. Richeter, B. Loock, P. Couleaud, C. Frochot, C. Charnay, G. Derrien, M. Smaihi, A. Sahmoune, A. Morere, P. Maillard, M. Garcia, J.-O. Durand, *Int. J. Pharm.* **2010**, *402*, 221 – 230.
[26] M. Maynadier, J. M. Ramirez, A. M. Cathiard, N. Platet, D. Gras, M. Gleizes, M. S. Sheikh, P. Nirde, M. Garcia, *FASEB J.* **2008**, *22*, 671 – 681.
[27] F. H. Schröder, J. Hugosson, M. J. Roobol, T. L. J. Tammela, S. Ciatto, V. Nelen, M. Kwiatkowski, M. Lujan, H. Lilja, M. Zappa, L. J. Denis, F. Recker, A. Berenguer, L. Maattanen, C. H. Bangma, G. Aus, A. Villers, X. Rebillard, T. van der Kwast, B. G. Blijenberg, S. M. Moss, H. J. de Koning, A. Auvinen, *N. Engl. J. Med.* **2009**, *360*, 1320 – 1328.
[28] H. U. Ahmed, C. Moore, M. Emberton, *Surg. Oncol.* **2009**, *18*, 219 – 232.

